Scientific Research

Bright Red Luminescence and Structural Properties of Eu³⁺ Ion Doped ZnO by Solution Combustion Technique

Sebastián López-Romero, María Jesús Quiroz-Jiménez, Manuel Hipólito García, Alfredo Aguilar-Castillo

Instituto de Investigaciones en Materiales, Universidad Nacional Autónoma de México Circuito Interior S/N Ciudad Universitaria México, México, D.F., México
Email: sebas@unam.mx

Abstract

Pure, and Europium ion doped Zinc oxide nanocrystals (ZnO:Eu³⁺) were synthesized by a solution combustion technique. The X-ray diffraction patterns (XRD) reveals the existence of the Eu_2O_3 phase. From the results of both, X-ray diffraction and photoluminescence spectra (PL) reveal that Eu³⁺ ions successfully substitute for Zn²⁺ ions in the ZnO lattice, moreover, when the amount of doped Europium was varied, this changes are showed in changes in the luminescence intensity. The PL is broad and a set of colors was emitted which originates from ZnO and the intra 4f transitions of Eu³⁺ ions. The existence of the Zn-O, Eu³⁺-O and O1s bonding energies were confirmed by X-ray photoelectron spectroscopy (XPS) technique. The samples morphology was registered by a scanning electron microscopy (SEM) technique, and reveals that Europium ions are present on the surface of the ZnO nanocrystals.
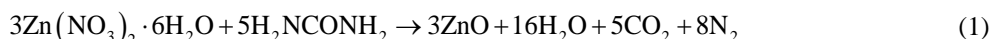
Keywords

1. Introduction

In the last few decades, the semiconductor zinc oxide (ZnO) with a wide band gap energy (3.37 eV) at room temperature and high exciton binding energy (60 meV) [1], has been used as host material for the doping of

rare-eart (RE) and transition metals (TM) ions, which exhibit optical and magnetic activity [2]-[6]. The RE-doped ZnO nanocrystals have an high potential to be used in integrated optoelectronic devices such as infrared and visible (blue, green, red) luminescent devices because they present a highly efficient luminescence even at room temperature [7]-[11]; the emission process is determined by the internal dynamics of the RE^{3+} electronics transitions governed by the relative energy of the 4f emitting level including the direct 4f-4f and indirect process $^5D_0 \rightarrow {}^7f_i$ with i = 0 - 4. From all the RE^{3+} ions, Eu^{3+} ion is the most representative and most widely studied and actually continue being used as dopant in many host compounds. Its color emission characteristic is the red color which is used in the fabrication of light emitting devises. Actually, it is possible to obtain and dope by several methods of the ZnO semiconductor in all your existent nanostructures: powders, nanowires, nanorods, nanobelts, nanonedles, nanorings, and nanoflowers [12]-[17]. Such methods are: radio frequency magnetron sputtering [4], spray pyrolysis deposition [18], hydrothermal synthesis [19], sol gel technique [20], thermal evaporation reactive [21], chemical vapor deposition [22], reactive magnetron sputtering [23], and solution combustion method [24]. The last method is considered as fast, simple, easy controlabilited, low cost and great scale production. In this work we synthesized ZnO intrinsic and Eu^{3+} doped ZnO (ZnO/Eu^{3+}) by a solution combustion method as a function of the Eu^{3+} ion concentration in wt% and after annealing at 900˚C by 24 h, also, the photoluminescence emission intensity of the $ZnO:Eu^{3+}$ as a function of the Eu^{3+} ion concentration is fited empirically by a exponential function and a phenomenological description and interpretation of the observed data is given.

2. Experimental

Undoped and Eu^{3+} ion doped ZnO nanocrystals $ZnO:Eu^{3+}$ were prepared by solution-combustion synthesis method as a function of the Eu^{3+} ion concentration in wt% using as source materials Zinc nitrate hexahydrated ($Zn(NO_3)_2 \cdot 6H_2O$) as oxidizer, urea (H_2NCONH_2) as fuel, and Europium chloride ($EuCl_3$) as dopant. In this process the follow redox chemical reaction stoichiometric oxidizer-fuel producing ZnO, H_2O vapor, CO_2, and N_2 is obtained:

$$3Zn(NO_3)_2 \cdot 6H_2O + 5H_2NCONH_2 \rightarrow 3ZnO + 16H_2O + 5CO_2 + 8N_2 \qquad (1)$$

The Equation (1) is obtained by taken in account the oxidizer/fuel molar radio (O/F = 1) required for a stoichiometric reactive solution which is determined by summing the total oxidicing and reducing valencies in the oxidizer compound and dividing it by the sum of the total oxidation and reducing valencies in the fuel compound [25]. Accordingly, for the complete combustion of Zinc nitrate-urea reactive solution, the molar ratio becomes 5/3, the molar balanced Equation (1) was obtained with this value. Using the atomic weight concept, the Equation (1) was translated to grams/mol and used to obtain 3 gr of ZnO powder for all the 0, 1, 3, 5, 7, and 10 wt% Eu^{3+} ion concentrations with respect to 3 gr of ZnO. From the translated grams/mol Equation (1) (no shown), 8.31 gr of $Zn(NO_3)_2 \cdot 6H_2O$, 3.68 gr of H_2NCONH_2 plus the numerous of grams corresponding to each Eu^{3+} ion concentration were mixing with 20 ml of H_2O and stirring vigourosly in a flask glas and after put on a hot plate at 500˚C, after a few minutes the reactive solution boils, foams, ignites, and burns with a incandescent flame at a approximate temperature of 1200˚C [26] producing 3 gr of ZnO powders approximately. After all the samples are annealing at 900˚C by 20 h. The $ZnO:Eu^{3+}$ samples thus obtained were structurally characterized by X-ray diffraction (XRD) technique using a Philips PW 1800 diffractometer with Cu kα radiation (1.5406 Å), XPS method was used to verify the Zn-O, Eu-O and O1s bonding energies (BE), the photoluminescence (PL) of the $ZnO:Eu^{3+}$ samples was studied by means of a spectrofluorometer FluoroMax-P that uses a xenon lamp as excitation source, The wavelength excitation was of 270 nm, and finally, the morphology of the $ZnO:Eu^{3+}$ powders was recorded using a scanning electron microscopy SEM) JEOL JSM 840 A.

3. Results and Discussion

3.1. Structural Characterization

Figure 1 shows the X-ray diffractograms of the $ZnO:Eu^{3+}$ powders as a function of the Eu^{3+} ion concentration and annealing at 900˚C by 20 h. From the XRD patterns, can be observed that all the diffraction peaks can be indexed to the majority phase hexagonal wurtzite tipe ZnO structure for all samples (JCPDS card #89-(102), moreover, for all the Eu^{3+} ion concentrations a little peak at $2\theta = 28.4°$ is observed, which is attributed to the (210) plane of the Eu_2O_3 minority phase (JPDS card #86-2476), Park *et al.* [27] reported diffraction peaks due to Eu_2O_3 after annealing the Eu^{3+} doped ZnO at temperatures higher 1000˚C in air and vacun conditions, no diffraction peaks were detected from other impurities. However, the intensity of the (101) peaks decrease with the
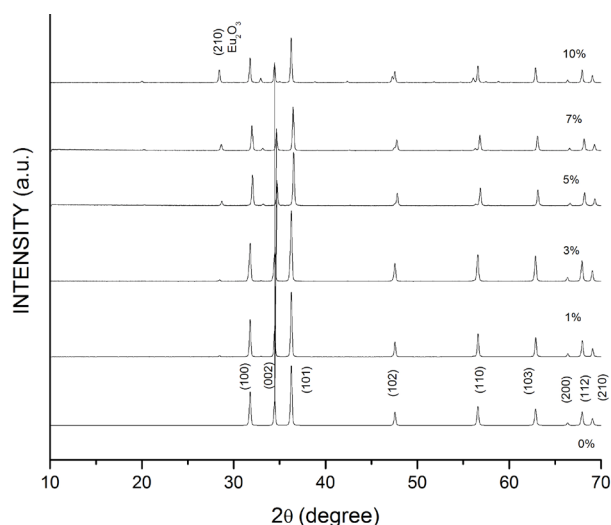
Figure 1. XRD patterns of the ZnO/Eu^{3+} samples as a function of the Eu^{3+} ion concentration in wt%.

increase in the Eu^{3+} concentration which create some disorder in the ZnO structure. This is further verify by the increase of he FWHM of the (101) peak with the Eu^{3+} concentration indicating a decrease in the crystallite size; effectively, using the Scherrer formula, the average crystallite size calculated from characteristic peak (101) was 41 nm for the ZnO intrinsic and decreased to 18 nm for the ZnO/Eu^{3+} samples doped with 10 wt% of Eu^{3+}. In addition, in **Figure 2**, are showed the diffraction patterns of the characteristic peaks (100), (002) and (101) of the doped ZnO/Eu^{3+} samples as a function of the Eu^{3+} ion concentration, it can be observed that the three peaks shifted towards a bigger 2θ vaue for 1, 3, and 5 wt% of Eu^{3+} concentration compared with the ZnO intrinsic, and further this peaks returned to the same position what that of the ZnO intrinsic, this change in the diffraction peaks towards a bigger 2θ value show a decrease of the lattice parameter and cell volume, this result is contrary to the results founded by another researchers [4] [28] [29] since the doping of the bigger size Eu^{3+} ion (effective ionic radio r_i = 9.74 nm) compared to that of the smaller Zn^{2+} ion (r_i = 7.40 nm) and therefore its incorporation in the ZnO lattice must lead to a increase in the cell parameters and volume, it is due to a low solubility of the Eu^{3+} ion in the ZnO lattice even for 1 wt% Eu^{3+} concentration, Yang et al. reported that the solution limit in the Eu^{3+} doped is below 0.2 wt% Eu^{3+} ion [10], this low solubility increase the yield of Eu$_2$O$_3$ species with increase of Eu^{3+} concentration at the ZnO nanocrystals surfaces [30] as is showed in the XRD diffraction patterns and at the SEM images showed in **Figure 4**.

3.2. XPS Analysis

To check the Eu^{3+} presence in the ZnO host, and its effect as a doping agent, on the surface chemical composition, XPS whole spectra of the ZnO:Eu^{3+} samples was obtained as a function of the Eu^{3+} ion concentration, **Figure 3** shows the binding energy (BE) for each ZnO:Eu^{3+} samples doped with the Eu^{3+} ion at 0, 1, 3, 5, 7, and 10 wt%, focusing in particular on the binding energies of the typical lines of O, Zn, and Eu. The O1s photoelectron peak showed a BE = 530.1 eV [31] [32], attributed to the lattice oxygen in a Zn-O-Zn network. With respect to the Zn ion presence the core-level photoelectron peaks showed a BE = 1021.5 eV corresponding to the core-level Zn2p$_{3/2}$ revealing the presence of Zn^{2+} ions in an oxide environment, the before analysis include to both undoped and Eu^{3+} ZnO doped. For all the Eu^{3+} ion concentrations, in your XPS spectrum respective there are two peaks in the Eu^{3+}3d region (1110 - 1170 eV) with BE = 1134.5 eV and 1164.3 eV corresponding to Eu^{3+}3d$_{5/2}$ and Eu^{3+}3d$_{3/2}$ respectively; both peaks are due to multiple spin-orbit interactions and are consistent with the reported values for Europium-coordinated ions which indicates that the oxidation states of Europium ions are trivalents for the ZnO:Eu^{3+} samples [29] [33]. Non other satelite peak can be seen on the XPS spectra.

3.3. Morphology of the ZnO/Eu³⁺ Samples

Figure 4 shows the SEM images of the as prepared ZnO:xEu^{3+} (x = 0, 1, 3, 5, 7, and 10 wt%) samples as a
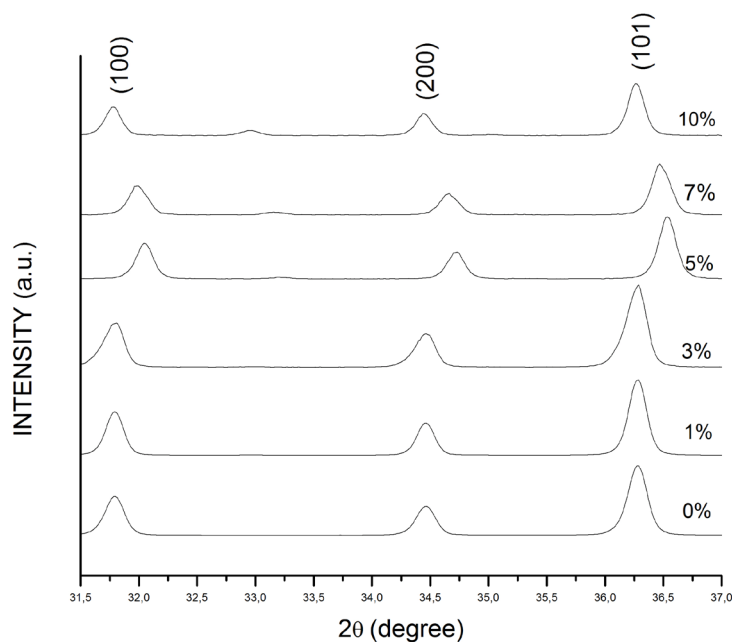
Figure 2. XRD patterns of the (100), (002) and (101) peaks of the ZnO; Eu^{3+} samples as a Function of the Eu^{3+} ion concentration in wt%.
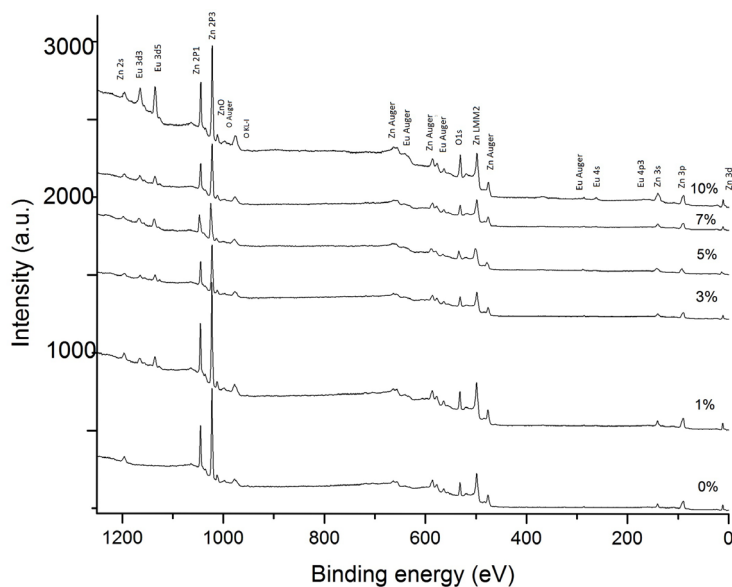

Figure 3. XPS spectra of the ZnO/Eu^{3+} samples as a fuction of Eu^{3+} concentration.

function of the Eu^{3+} ion concentration in wt% and after annealing at 900°C by 24 h. As can be observed, there are not clear morphological differences between undoped and Eu^{3+} doped samples indicating that the Eu^{3+} dopant in the ZnO host do not affect its morphology of the ZnO:Eu^{3+} nanocrystals. The grains of the ZnO have a mean large about 0.6 µm. Moreover, it can be seen that Eu^{3+} crystallites are adhered to the ZnO surface increasing with the Eu^{3+} ion concentration.

3.4. Photoluminescence Properties

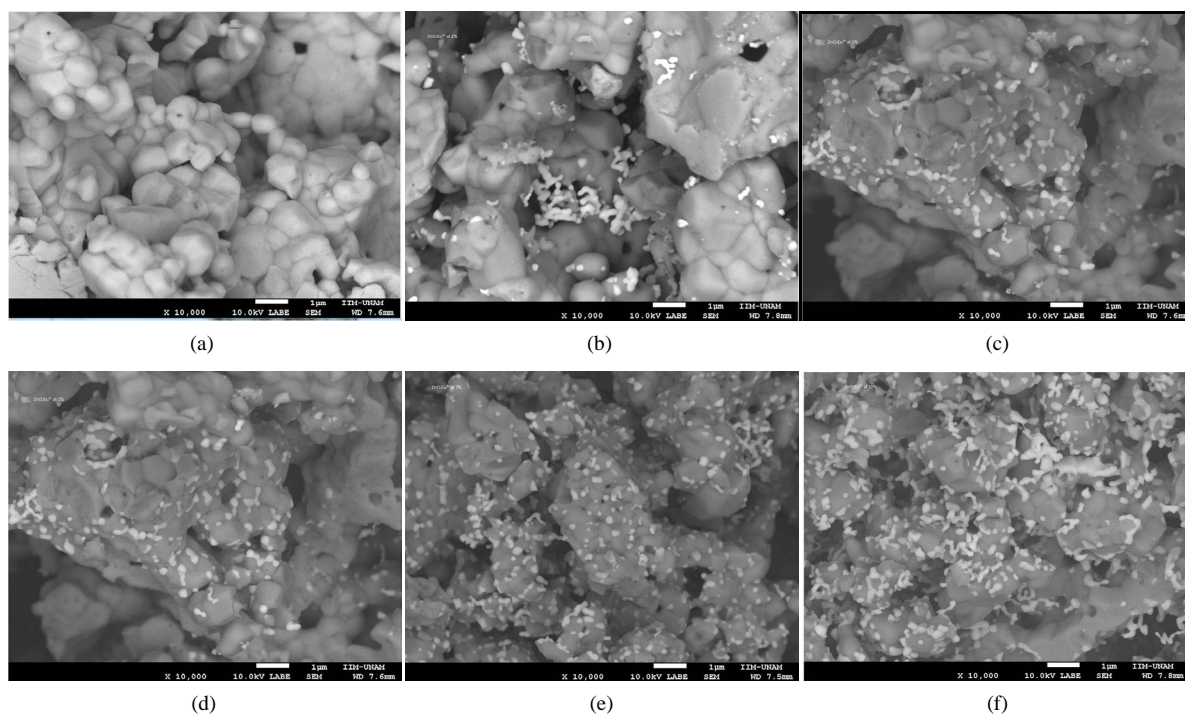**Figure 5** shows the room temperature photoluminescence spectra (PL) of the ZnO:Eu^{3+} nanocrystals as a

Figure 4. SEM images of the ZnO/Eu^{3+} samples as a function of the Eu^{3+} Concentration. (a) 0%; (b) 1%; (c) 3%; (d) 5%; (e) 7%; (f) 10%.
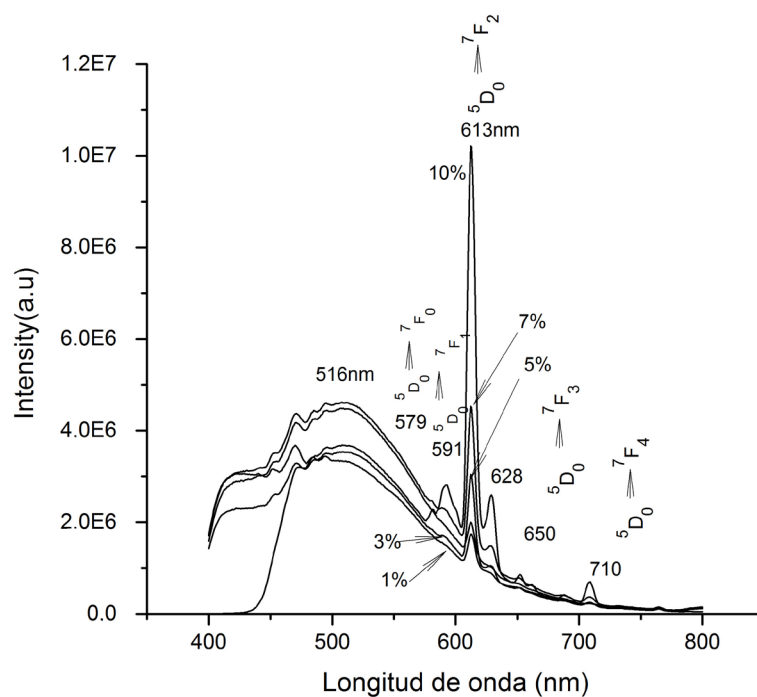

Figure 5. Room temperature photoluminescence spectra of the ZnO:Eu^{3+} samples as a function of the Eu^{3+} ion concentration irradiated with a excitation wavelength of 270 nm.

function of the Eu^{3+} ion concentration in wt% and after annealing at 900°C by 24 h, the samples were irradiated with an excitation wavelength of 270 nm (in the UV range). It is observed that the ZnO:Eu^{3+} samples doped with

1, 3, 5, 7 and 10 wt% are all alike: they present a green broad emission band from 400 nm to 600 nm centered about 516 nm, this band is due to the intrinsic defects emission of ZnO host. however, in addition to the broad band characteristic of defects in ZnO appear the photoluminescence spectra of the Eu^{3+} doped powders: effectively, the sharp peaks in 579, 591, 613, 618, 650 and 770 nm are related to the direct intra-4f transitions in Eu^{3+} ions $^5D_0 \rightarrow {}^7F_j$ (j = 0, 1, 2, 3, 4), the most intense emission is associated to the $^5D_0 \rightarrow {}^7F_2$ emission in the red spectral region (613 nm) and is due to an allowed electric-dipole transitions with inversion antisymmetry [19], which results in a large transition probability in the crystal field; in our case this emission is split in two components of 613 and 618 nm, theoretically, the $^7F_2$ level gives three crystal field levels of A1 and 2E with $3C_v$ symmetry, because A1 and one of two E levels have close energy levels, two emission peaks (A1 and E at 613 and 618 nm) can be overlapped in the PL spectra [34] [35]. The peak at 591 nm is due to the $^5D_0 \rightarrow {}^7F_1$ transition, is an allowed magnetic-dipole transition, if the Eu^{3+} ion is situated in a symmetry center in the ZnO matrix, electric-dipole transitions between the $4f^6$ levels are strictly forbidden by the Laporte selection rule (equal parity) while the magnetic-dipole is allowed. Thus, the intensity ratio of $^5D_0 \rightarrow {}^7F_2$ to $^5D_0 \rightarrow {}^7F_1$ transition known as symmetry ratio can provide information about the quality structural of the material [35] [36]. The symmetry ratio in our material about 8 indicating low inversion symmetry when the Eu^{3+} ion is incorporated into hexagonal ZnO host by substitution on Zn sublattice. The peak at 579 nm is due to the forbidden $^5D_0 \rightarrow {}^7F_0$ transition due to the same total angular momentum, indicating that some Eu^{3+} ions possibly occupy other sites as interticial sites [37] [38]. **Figure 6** shows the integrated emission intensity variation of the $^5D_o \rightarrow {}^7F_2$ transition as a function of the Eu^{3+} ion concentration, the empiric graphic was fited, to the exponential function $I(\%) = 1.3E6 * e^{0.23\%}$ where % is the Eu^{3+} ions concentration, the solid curve in **Figure 5** represents the fit to the experimental data, the integrated intensity increases as an exponential function as the doping concentration increase which indicates the enhanced energy transfer between the ZnO host and activator Eu^{3+} ions. The concentration Quenchin effects do not appear in this concentration range.

4. Conclusion

In this work undoped and Eu^{3+} doped ZnO nanocrystals were synthesized by a solution combustion technique. From XRD studies, the ZnO:Eu^{3+} structure resulted in the hexagonal wurtzite ZnO structure for all the Eu^{3+} ion concentrations; and also showed the existence of the Eu_2O_3 phase mixed with the ZnO phase. The effect of Eu^{3+} doping percentage on the nanocrystals showed that with increasing doping percentage, disorder in the nanocrystals increases. From the XPS spectra, the oxidation states of the Eu ions are trivalent for the Eu^{3+} doped ZnO nanocrystals. Solution combustion synthesized Eu^{3+} doped ZnO nanocrystals are found to emit red and green
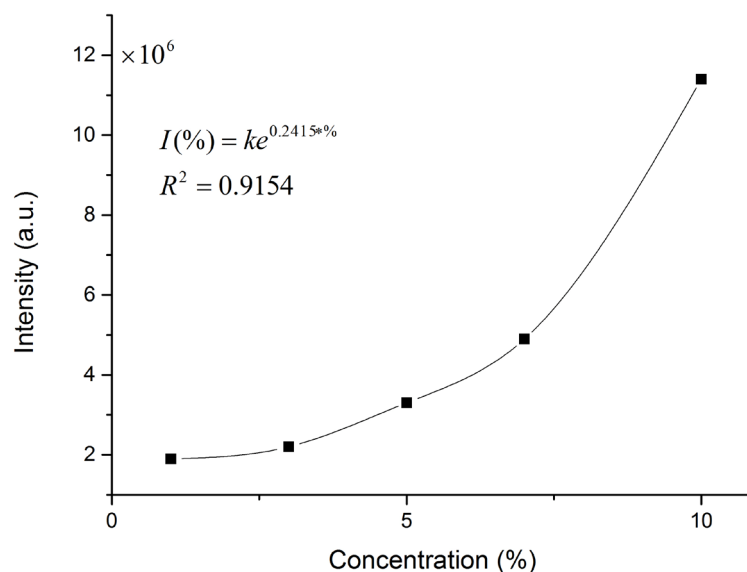

Figure 6. Fit of the intensity emission integrated of the transition $^5D_0 \rightarrow {}^7F_2$ as a funtcion of the Eu^{3+} ion concentration in wt%.

light. The intensity of the emission was related to doping concentration by means of an exponential fit.

Acknowledgements

References

[1] Kashai, A. and Kaur, D. (2011) Pulsed Laser Deposition of Transparent ZnO/MgO Multilallers. *Journal of Alloys and Compounds*, **509**, 200-205.

[2] Senthilkumaar, S., Rajendran, K., Banergee, S., *et al*. (2008) Influence of Mn Doping on the Microstructure and Optical of ZnO. *Materials Science in Semiconductor Processing*, **11**, 6-12. http://dx.doi.org/10.1016/j.mssp.2008.04.005

[3] Lang, J.H., Hang, O., Yang, J., *et al.* (2010) Fabrication and Optical Properties of Ce-Doped ZnO Nanorods. *Journal of Applied Physics*, **107**, Article ID: 074302. http://dx.doi.org/10.1063/11.3318613

[4] Tan, Y.S., Fang, Z.B., Chen, W., *et al*. (2011) Structural, Optical and Magnetic Properties of Eu-Doped ZnO Films. *Journal of Alloy and Compounds*, **509**, 6321-6324.

[5] Cambers, S.A., Schwaritz, D.W. and Liu, W.K. (2007) Growth, Electronic, and Magnetic Properties of Doped ZnO Epitaxial and Nanocrystalline Films. *Applied Physics A*, **88**, 1-5.

[6] Peres, M., Cruz, A., Ferreira, S., *et al.* (2007) Optical Studies of ZnO Nanocrystals Doped with Eu^{3+} Ions. *Applied Physics A*, **88**, 129-133. http://dx.doi.org/10.1007/s00339-007-3941-9

[7] Liu, Y.S., Luo, W.Q., Li, R.F., *et al*. (2007) Spectroscopic Evidence of the Multiple-Site Structure of Eu^{3+} Ions Incorporated in ZnO Nanocrystals. *Optics Letters*, **32**, 566-568.

[8] Yukihara, E.G., Milliken, E.D., Oliveira, L.C., *et al*. (2013) Systematic Development of New Thermoluminescence and Optically Stimulated Luminescence Materials. *Journal of Luminescence*, **133**, 2003-2210.

[9] Gomez, M.A., Valeria, M.E.G., Queiruga, J.F., *et al*. (2013) Comparative Study of Structural and Optical Properties of ZnO Nanostructures Prepared by Three Different Aqueous Solution Methods. *Materials Chemistry and Physics*, **142**, 325-332.

[10] Yang, C.-C., Cheng, S.-Y., Lee, H.-Y., *et al.* (2006) Effects of Phase Transformation on Photoluminescence Behavior of ZnO:Eu Prepared in Different Solvents. *Ceramics International*, **32**, 3741.

[11] Jiang, N., Ye, S. and Yang, B. (2013) Microstructure of Yb and Li Co-Doped ZnO by Electron Microscopy. *Materials Chemistry and Physics*, **142**, 37-43. http://dx.doi.org/10.1016/j.matchemphys.2013.06.027

[12] Wang, Z.L. (2009) ZnO Nanowires and Nanobelt Platform for Nanotechnology. *Materials Science and Engineering*, **64**, 33-71. http://dx.doi.org/10.1016/j.mser.2009.02.001

[13] Yang, J.H., Li, X., Lang, J.H., *et al.* (2011) Synthesis and Optical Properties of Eu-Doped ZnO Nanosheets by Hydrothermal Method. *Materials Science in Semiconductor Processing*, **14**, 247-252. http://dx.doi.org/10.1016/j.mssp.2011.04.002

[14] Sadhu, S., Zen, T. and Patra, A. (2007) Shape Controlled Synthesis and Luminescence Properties of $ZnO:EU^{3+}$ Nanostructures. *Chemical Physics Letters*, **440**, 121-124. http://dx.doi.org/10.1016/j.cplett.2007.04.015

[15] Ishizumi, A., Takahashi, Y., Yamamoto, A., *et al.* (2008) Fabrication and Optical Properties of Eu^{3+}-Doped ZnO Nanospheres and Nanorods. *Materials Science & Engineering*, **146**, 212-215.

[16] Wang, Z.I. (2007) Novel Nanostructures of ZnO for Nanoscale Photonics, Optoelectronics, Piezoelectronics, Piezoelectricity and Sensing. *Applied Physics A*, **88**, 7-15. http://dx.doi.org/10.1007/s00339-007-3942-8

[17] López-Romero, S., Santiago, P. and Mendoza, D. (2011) Hydrothermal Synthesis and Characterization Structural of Flower-Like ZnO Nanostructures. *Advanced Science Letters*, **4**, 1-5.

[18] Panatarani, C., Lenggoro, I.W. and Okuyama, K. (2004) The Crystallinity and the Photoluminescent Properties of Spray Pyrolized ZnO Phosphor Containing Eu^{2+} and Eu^{3+} Ions. *Journal of Physics and Chemistry of Solids*, **65**, 1843-1847.

[19] Zhong, M.Y., Shang, G.Y., Li, Y.J., *et al.* (2007) Synthesis and Luminescence Properties of Eu^{3+}-Doped ZnO Nanocrystals by a Hydrothermal Process. *Materials Chemistry and Physics*, **106**, 305-309. http://dx.doi.org/10.1016/j.matchemphys.2007.06.007

[20] Saleh, W.R., Saeed, N.M., Twej, W.A., *et al.* (2012) Synthesis Sol-Gel Derived Highly Transparent ZnO Thin Films

for Optoelectronic Applications. *Advances in Materials Physics and Chemistry*, **2**, 11-16. http://dx.doi.org/10.4236/ampc.2012.21002

[21] Jia, W.Y., Monge, K. and Fernandez, F. (2003) Energy Transfer from the Host to Eu^{3+} in ZnO. *Optical Materials*, **23**, 27-32. http://dx.doi.org/10.1016/S0925-3467(03)00054-5

[22] Protasova, L.N., Rebrov, E.V., Choy, K.L., *et al.* (2011) ZnO Based Nanowires Grown by Chemical Vapour Deposition for Selective Hydrogenation of Acetylene Alcohols. *Catalysis Science & Technology*, **1**, 768-777. http://dx.doi.org/10.1039/c1cy00074h

[23] Hong, R.J., Huang, J.B., He, H.B., *et al.* (2005) Influence of Different Post-Treatments on the Structure and Optical Properties of Zinc Oxide Thin Films. *Applied Surface Science*, **242**, 346-352. http://dx.doi.org/10.1016/j.apsusc.2004.08.037

[24] Devi, S.K.L., Kumar, K.S. and Balakrishnan, A. (2011) Rapid Synthesis of Pure and Narrowly Distributed Eu Doped ZnO Nanoparticles by Solution Combustion Method. *Materials Letters*, **65**, 35-37.

[25] Miamani, T. and Patil, K.C. (2001) Solution Combustion Synthesis of Nanoscale Oxides and Their Composites. *Materials Physics and Mechanics*, **4**, 134-137.

[26] Patil, K.C., Hegde, M.S., Rattan, T. and Aruna, S.T. (2008) Chemistry of Nanocrystalline Oxide Materials: Combustion Synthesis, Properties and Applications. World Scientific Publishing Company, New Jersey.

[27] Van Park, Y.R., Jan, J.I., Kwar, M.G., *et al.* (1998) Effect of Coupling Structure of Eu on the Luminescence Characteristics for $ZnO/EuCl_3$ Phosphors. *Applied Physics Letters*, **72**, 668. http://dx.doi.org/10.1063/1.120833

[28] Luo, L., Gong, L., Liu, Y.F., *et al.* (2010) Enhanced Ultraviolet Lasing From Europium-Doped Zinc Oxide Nanostructures. *Optical Materials*, **32**, 1066-1070.

[29] Phuruangrat, A., Yayapao, O., Thongtem, T. and Thongtem, S. (2014) Synthesis and Characterization of Europium-Doped Zinc Oxide Photocatalyst. *Journal of Nanomaterials*, **2014**, Article ID: 367529. http://dx.doi.org/10.1155/2014/367529

[30] Petersen, J., Brimont, C., Gallart, M., *et al.* (2010) Correlation of Structural Properties with Energy Transfer of Eu-Doped ZnO Thin Film Prepared by Sol-Gel Process and Magnetron Reactive Sputtering. *Journal of Applied Physics*, **107**, Article ID: 123522. http://dx.doi.org/10.1063/1.3436628

[31] Baek, S., Song, J. and Lim, S. (2007) Improvement of the Optical Properties of ZnO Nanorods by Fe Doping. *Physica B*, **399**, 101-104.

[32] Armelao, L., Bottaro, G., Pascoline, M., *et al.* (2008) Structure-Luminescence Correlations in Europium-Doped Sol-Gel ZnO Nanorods. *The Journal of Physical Chemistry C*, **112**, 4049-4054.

[33] Du, Y.-P., Zhang, Y.-W., Sung, L.-D., *et al.* (2008) Efficient Energy Transfer in Monodisperse Eu-Doped ZnO Nanocrystals Synthesized from Metal Acetylacetonates in High-Boiling Solvents. *The Journal of Physical Chemistry C*, **112**, 12234-12241. http://dx.doi.org/10.1021/jp802958x

[34] Ursaki, V., Rusu, E., Zalamai, V., *et al.* (2004) Photoluminescence of Eu Doped ZnO Structures. *Proceeding of SPIE*, **5822**, Chisinau, 3 May 2004. http://dx.doi.org/10.1117/12.612229

[35] Fujihara, S.O., Suzuqui, A. and Kimura, T. (2003) Ga-Doping Effects on Electrical and Luminescent Properties of ZnO: (La,Eu) of Red Phosphor Thin Films. *Journal of Applied Physics*, **94**, 2411.

[36] Qi, J.F., Matsumoto, T., Tanaka, M., *et al.* (2000) Europium Silicate Thin Films on Si Substrates Fabricates by a Radio Frequency Sputtering Method. *Journal of Physics D*: *Applied Physics*, **33**, 2074.

[37] Ningthoujam, R.S. and Nanoci, J. (2008) Dispersible Li^+ and Eu^{3+} Co-Doped Nanocrystalline: ZnO Luminescence and EPR Studies. *Journal of Nanoscience and Nanotechnology*, **8**, 3059. http://dx.doi.org/10.1166/jnn.2008.152

[38] Chen, P.L., Ma, X.Y. and Yang, D.R. (2007) ZnO:Eu Thin Films: Sol-Gel Derivation and Strong Photoluminescence from $^5D_0 \rightarrow ^7F_0$ Transition of Eu^{3+} Ions. *Journal of Alloys and Compounds*, **431**, 317-320.

Scientific Research Publishing (SCIRP) is one of the largest Open Access journal publishers. It is currently publishing more than 200 open access, online, peer-reviewed journals covering a wide range of academic disciplines. SCIRP serves the worldwide academic communities and contributes to the progress and application of science with its publication.

Other selected journals from SCIRP are listed as below. Submit your manuscript to us via either submit@scirp.org or Online Submission Portal.